

# Luminescence detection of phase transitions in crystals and nanoparticle inclusions

P.D. Townsend

*Science and Technology, University of Sussex, Brighton, BN1 9QH, UK,  
e-mail: p.d.townsend@sussex.ac.uk*

B. Yang

*Physics Department, Beijing Normal University, Beijing, 100875, China,  
e-mail: yangbr@bnu.edu.cn*

Y. Wang

*School of Materials Science and Technology, China University of Geosciences, Beijing, 100083, China,  
e-mail: wyfemail@gmail.com*

Recibido el 12 de octubre de 2007; aceptado el 9 de agosto de 2008

Luminescence measurements are extremely sensitive to variations in structural environment and thus have the potential to probe distortions of fluorescence sites. Changes can be monitored via luminescence efficiency, emission spectra or excited state lifetimes and these factors are influenced by the local neighbourhood around the emission site, and therefore by structure, composition, pressure and temperature. A rarely exploited approach for condensed matter has been to use the changes in luminescence responses during heating or cooling of a material to provide a rapid survey to detect the presence of phase transitions. One can often differentiate between bulk and surface effects by contrasting results from radioluminescence for bulk responses, and cathodoluminescence or photoluminescence for surface effects. One expects that discontinuous changes in optical parameters occur during temperature changes through phase transitions of insulating materials. In practice, optical signals also exist from surface states of fullerenes and high temperature superconductors etc which identify the presence of structural or superconducting transitions. Numerous examples are cited which match standard documented transitions. Interestingly, many examples show the host signals are strongly sensitive to impurity phase transitions from inclusions such as nanoparticles of water,  $N_2$ ,  $O_2$  or  $CO_2$ . Recent luminescence data reveal many examples of new transitions, hysteresis and irreversible changes. The signals equally respond to relaxations of a structure and surprisingly indicate that in some materials, such as  $SrTiO_3$  or  $ZnO$ , ion implantation of the surface triggers relaxations and phase changes throughout the bulk of the material. Luminescence routes to detect phase transitions are powerful tools but have a tiny literature and so the subject is ideal for rapid exploitation and development.

**Keywords:** Phase transitions; nanoparticle inclusions; luminescence.

La espectroscopía de luminiscencia es extremadamente sensible a las variaciones en la estructura de los materiales, de tal forma que puede ser utilizada para investigar distorsiones en sitios fluorescentes. Dichos cambios pueden ser monitoreados a través de la eficiencia de la luminiscencia, espectros de emisión o tiempos de vida de estados excitados; estos factores son afectados por el medio que rodea el sitio de emisión, y por lo tanto su estructura, composición, presión y temperatura. Un método que ha sido poco explotado en estudios de la materia condensada es usar la respuesta luminiscente durante el calentamiento o enfriamiento de un material a manera de inspección rápida para detectar la presencia de transiciones de fase. Usualmente es posible discernir entre los efectos del material en volumen y la superficie contrastando los resultados que se obtienen de la radioluminiscencia en el caso del sustrato y la catodoluminiscencia o fotoluminiscencia para los efectos de superficie. Es de esperarse que ocurran cambios discontinuos en los parámetros ópticos durante variaciones de temperatura a través de transiciones de fase en materiales aislantes. De hecho, también existen señales ópticas de estados superficiales de fulerenos y superconductores bajo altas temperaturas, entre otros, las cuales identifican la presencia de transiciones estructurales o de la superconductividad. Numerosos ejemplos muestran que las señales ópticas del material son altamente sensibles a transiciones de fase de impurezas como nanopartículas de agua,  $N_2$ ,  $O_2$  o  $CO_2$ . Varios resultados recientes de luminiscencia revelan muchos ejemplos de nuevas transiciones, histéresis y cambios irreversibles. Las señales responden igualmente a relajaciones de alguna estructura e indican de manera sorprendente que en algunos materiales como  $SrTiO_3$  o  $ZnO$ , la implantación iónica de la superficie activa relajaciones y cambios de fase hacia todo el volumen. Los métodos de luminiscencia para detectar transiciones de fase son herramientas poderosas pero poseen una bibliografía incipiente, de manera que el tema es ideal para ser explotado y desarrollado rápidamente.

**Descriptores:** Transiciones de fase; inclusiones nanométricas; luminiscencia.

PACS: 64.60.-I; 64.70.Nd; 78.60.-G; 71.55.Jv

## 1. Introduction

Phase transitions between different states from solid to liquid to gas are familiar features. Whilst visually less obvious, there are a multitude of examples in which solids undergo structural changes, normally between different crys-

tallographic phases [1]. Most such transitions are reversible although it is not uncommon to have hysteresis effects. Structural changes which involve different phases may equally include those between crystalline to amorphous phases, with the quartz to amorphous silica glass as a familiar example. Interdiffusion between related compounds may also occur, as

in thermal and radiation treatments of mixed feldspars. In the case of doped materials there are inherent stresses and/or ionic charge differences between the host and impurity materials which generate stresses or charge imbalance that are accommodated in a variety of ways. In some cases impurities are located at normal lattice sites but introduce local distortions. In other examples the stress fields are so strong that there is precipitation of new phases which can either involve the ions of the host material or be a totally independent inclusion phase. Historically such precipitate phases might have been seen as undesirable, but current interests in production and control of nanoparticles now implies that such impurity phases may actually be the main objective of the sample treatments. Surface and bulk material will also differ in the details of their bonding and the differences in relaxation options can lead to surface reconstruction of a lattice which may extend some depth into the solid. Surfaces and grain boundaries are favourable regions for the influx of impurities, such as water or solvents, and these in turn may result in impurity phases separate from the host material. Detection of phase changes is thus a complex problem which calls for a range of analysis techniques. Not all of the methods can detect all types of phase and so there is an opportunity to advance new methods which allow rapid surveys to locate temperature or pressure conditions which generate phase changes. Once identified, the more specific methods can be applied to give detailed lattice parameter data and crystallographic phase information.

Well established methods include determination of lattice structures, as sensed by X-ray, neutron or electron diffraction. The lattice parameters, crystallography and unit cell structures so derived are well quantified for high quality bulk materials. However, the methods are relatively time consuming and not always well suited to detailed and rapid monitoring of changes with temperature, or the previously mentioned problems of relaxations in the near surface regions, inclusions, precipitates or hysteresis. It is important to note that many insulating materials undergo structural radiation damage during X-ray characterization, and the damage will modify the parameters, including the phase. Alkali halides, many silicates and organics respond in this way [2,3]. Such events are most obvious in the region of the surface and so there can be differences between bulk and powder or nanoparticle material. Further, powder structures may differ in detail as a function of particle size, as is documented for nanoparticle production [4-6]. The energy associated with phase changes can be monitored via differential thermal analysis, but in the cases where there are secondary or precipitate phases, including nanoparticles, the energy changes may be difficult to isolate if the microphase variants occupy only a tiny percentage of the total material. For well established crystals minor impurity phase variations can be recognised, but with the introduction and expansion of materials with more exotic properties, as used in photonics, it may be difficult to initially separate problems of thin film or crystal growth from intrinsic properties of the host lattice. So once again there is an interest in rapid survey methods prior to detailed analyses.

In the case of optical materials immediately obvious methods include measurements of the optical band gap, dielectric constants, refractive indices and birefringence, or Raman signals [e.g. 7-14]. Photoluminescence and cathodoluminescence have a similar long history [e.g. 15-17] and examples include not only inorganic and semiconductor crystals but also the phase transitions from crystalline to smectic to isotropic transitions of liquid crystals [14]. Work with polymers has been reported [18] but often the examples involve a broad temperature range, rather than a sharp transition event. Luminescence is of course a valuable and direct monitor of relaxations and phase changes, not least because of the high sensitivity with which one can record spectral information. Numerous studies have exploited the site sensitive transition energies (and lifetimes) of rare earth ions embedded in a lattice and phase transitions of the host are reflected by discrete shifts in these properties [10-12]. Nevertheless, the presence of the rare earth probe can itself modify the lattice stability, not least by inducing precipitate phases which include the rare earth ions. Luminescence emission lines of other dopants, such as chromium, have equally been valuable, as in ruby, to characterise temperature and pressure changes in the host material.

The existing literature of using luminescence to detect phase changes has established the potential of the method but few authors have used the wider approach of detecting emission spectra during heating or cooling of a sample in order to make initial surveys of possible phase changes. The current review will emphasise the information which can be revealed, and substantiate some of the claims from recent data. Although the examples used here are primarily from work at Sussex it will be seen that the range of materials which are amenable to these luminescence surveys of phase transition type events is considerable. Indeed, it is surprising that the literature is so sparse since the technology for the luminescence method has existed for several decades.

## 2. Experimental techniques

Excitation of luminescence can be achieved in a variety of ways. Bulk excitation resulting from X-ray irradiation (RL) can differ from near surface data. For surfaces one has partial control of the excitation depth by varying the electron energy in cathodoluminescence (CL), but the greatest fraction of the energy deposition occurs within  $\sim 35\%$  of the electron range. By contrast, ion beam luminescence (IBL) with light ions generates similar ionisation events as for CL but with a different depth distribution. IBL has some attractive alternative features as one can change the depth and rate of energy transfer by varying the ion energy and implant species [19]. With molecular ions ( $H_2^+$  or  $N_2^+$  etc) one generates extremely high excitation density along the track of the dissociating molecules. Photoluminescence (PL) can be wavelength selective in the choice of luminescence site that is stimulated (e.g. intrinsic defects or nanoparticles). For rare earth ions changes in wavelength offer the opportunity for site selec-

tive excitation as the transition energies are defined by site symmetry, perturbed by local imperfections and distortions induced by phase changes. Hence one can separate different types of phase transition. For semiconductor samples electroluminescence (EL) is also feasible. Finally, one can use thermoluminescence (TL) to study charge release after irradiation. For temperature scans in phase transition assessments there may be an element of TL signals mixed in with the changing equivalent signals of RLTL, CLTL, IBLTL, PLTL or ELTL. This is less of a problem for measurements in cooling cycles. Although there are not yet literature examples, we have noted that the simultaneous combination of excitation methods (*e.g.* RL + CL) can reveal new signals. This is slightly unexpected as the depth scales of the two methods are many millimetres for RL but only microns for CL. Reasons for the changed responses have not yet been discussed. By contrast the non-additive combination of a mixture of IBL and PL is less surprising since both methods can be limited to near surface regions and IBL forms transient defects (and can stimulate surface relaxations and phase transitions) which can be probed by the optical excitation. Our unpublished data with such combined excitation methods suggests further investigations of this complex situation would be very fruitful.

Excitation is not confined to steady state methods and property differences can be greatly enhanced by the use of pulsed excitation and studies of signal decay or measurement of excited state lifetime. This is valuable if the sample emission spectra are similar in different phases as emphasis must be placed on intensity and lifetime changes. In the case of inclusions within a host material the host emission spectra may not change significantly when the inclusions or nanoparticles undergo a phase transition. This does not mean the two types of event are independent as there are very long range defect interactions, both from charge interactions and pressure. At low temperature exciton electron-hole pair coupling up to >50 neighbouring shells has been documented in some cases [2]. The volume of the host lattice modified by impurities or inclusions is thus far greater than the volume of the inclusion or defect concentration. Unfortunately many discussions of imperfections and luminescence sites are phrased in terms of isolated lattice sites but our perception of the scale of long range interactions has increased with time and in reality no region of a crystal is truly perfect and free from the influence of imperfections [20,21]. Host signals can alter dramatically in intensity as the result of phase changes of inclusions, for example with garnets [22] or zircon [23]. Sensitive spectral changes in the host lattice from inclusions can also be monitored via line or broad band transitions, for example by using rare earth or Cr dopant probes [24]. Several examples will be cited later. Similarly the spectrum can remain unaltered but there will be discrete changes in emission lifetime and we have noted such effects in CL of some minerals, even though there were only minor variations in signal intensity. Lifetime discrimination of different emission sites, including phase changes, is well established and one notes

that, in the rapidly developing field of optical biopsy, fluorescence lifetime imaging is a particularly powerful method to resolve differences between healthy and diseased tissue [25]. This biological "phase transition" between healthy and modified tissue has similarities in that the intensity, emission spectra, lifetime etc of the signals differ between the variants and the signals are sensitive to long range effects. Similarly, botanical examples of water content in a leaf show changes in emission spectral components, for example with different lifetimes and intensity for wet and dry leaves. The equipment and methodology developed for biological objectives can equally be utilised in condensed matter studies, such as those seeking separation of differences in grain size dependent phase transitions and since the optical biopsy is becoming a major field there will be developments in equipment which may be ideal for the condensed matter studies as well.

Temperature control in a heating or cooling cycle is most conveniently a linear function of time; hence the equipment requirements are precisely those of thermoluminescence. A note of caution is that in dosimetry TL very high heating rates (degrees/sec) are used and the sample temperature and thermocouple recorded temperatures differ very considerably [26,27]. It is not a problem for dosimetry but it is essential to use low heating rates (degrees/min) and careful and accurate temperature corrections for the data being used to study phase transitions. Indeed the inverse approach has been very successful and one can use the signal from a phase transition to calibrate temperature lag of a TL system [28,29].

A major strength of a luminescence technique is that signal detection can be extremely sensitive when using photocathode type detectors, which benefit from having time resolution faster than a nanosecond. For surveys of phase detection it is almost essential to simultaneously record the entire emission spectra during a dynamic temperature run. This places greater demands on the equipment design. For example, the Sussex system, from which many of our examples are drawn, was constructed in 1990 and used a pair of diffraction gratings blazed for different spectral regions plus a pair of photon imaging tubes with photocathodes to cover either the UV/blue or the extended red regions. Since 1990 improvements with CCD detectors mean that the differences in sensitivity between photon imaging tubes and CCDs are often much less. In a modern design CCD detection might be a preferred alternative, not least as a CCD has sensitivity to longer wavelengths. CCD detection may not be suitable in fast lifetime resolved studies and these benefit from the fast responses of photomultiplier detection. Monochromatic detection is acceptable if data are recorded sequentially at a series of fixed different temperatures or wavelengths.

In summary it appears that detection equipment requirements are very similar to those needed in any serious study of thermoluminescence where attention has been paid to the recording of wavelength multiplexed emission spectra. Phase transition studies could therefore be widely addressed with existing equipment.

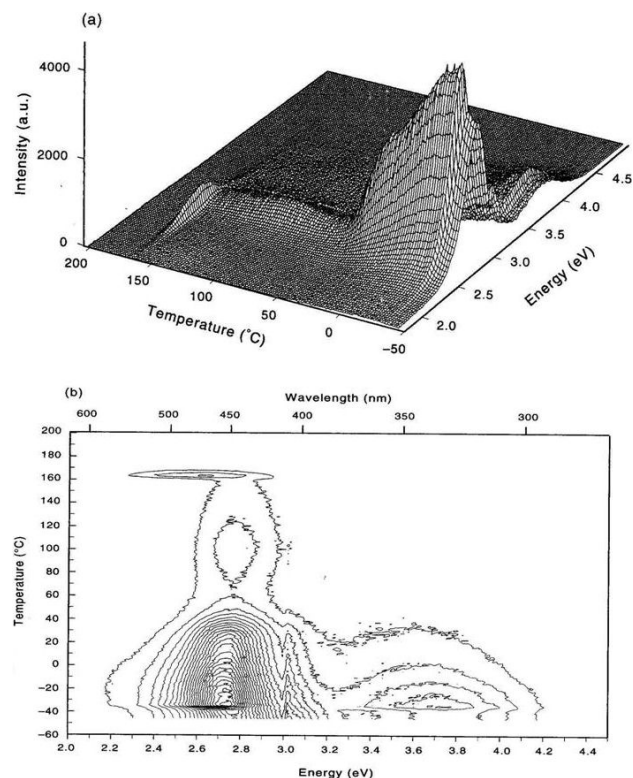


FIGURE 1. Isometric and contour views of thermoluminescence spectra of ammonium bromide.

### 3. Examples of luminescence signals resulting from phase changes

#### 3.1. Spectra

Luminescence detectors are sensitive and offer signals in a variety of ways. For example the emission spectra, intensity and lifetimes all respond to phase changes not only of the host material but also of inclusions, stress and surface effects. Figure 1 shows an isometric plot and a contour map of RLTL from ammonium bromide [28]. Because the sample is being heated there are temperature differences between the measured heater strip temperature and the emitting face of the sample. The figure is plotted in terms of the monitored temperature and correction factors will be discussed later as a function of heating rate. With this caveat one can easily detect the two documented phase transitions in this temperature range [9]. The lower transition near  $-38^{\circ}\text{C}$  (235 K) has a small intensity step and a wavelength shift of the main emission band. The higher transition (here seen at  $\sim 160^{\circ}\text{C}$  instead of  $138^{\circ}\text{C}$ ), has a far more obvious change in emission wavelength. The contour plot emphasises the two transitions via the shifts in emission wavelengths, most obviously so for the higher temperature transition. In addition to the wavelength shift the high density of contour lines near a transition temperature gives the appearance of a dark band of horizontal contour lines when the spectrum is similar in the two phases, as for the  $-38^{\circ}\text{C}$  event.

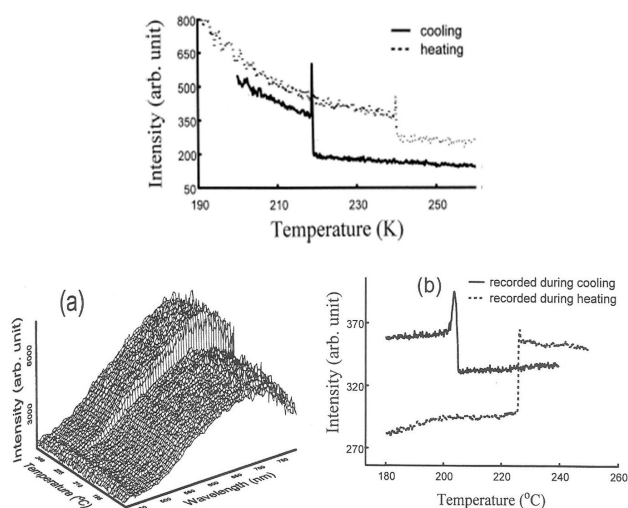


FIGURE 2. Luminescence intensity and spectra from  $\text{KNbO}_3$  during heating and cooling.

Rather than use the intrinsic broad band signals one can probe lattice changes with more subtlety by the use of line spectra, particularly from rare earth ions. For example in an earlier example of Sm doped  $\text{SrF}_2$  the rare earth ions show a number of narrow emission lines which change in wavelength and overall relative intensities as a function of temperature and pressure as these parameters modify the local crystal field [10]. In particular there is a line feature near  $14,353\text{ cm}^{-1}$  ( $696.7\text{ nm}$ ), which discontinuously shifts to  $\sim 15,350\text{ cm}^{-1}$  when the crystal undergoes a pressure induced phase change. The host  $\text{SrF}_2$  switches between two phases labelled  $\alpha$  and  $\beta$  at a pressure near 2GPa. This is informative as this emission line indicates that there is a distinct hysteresis in the pressure induced reversal between the two phases, with transition occurring at  $\sim 5\text{ GPa}$  during pressure increases but reversing at  $\sim 2\text{ GPa}$  during pressure reduction. By contrast an example for pressure changes noted via Eu signals in  $\text{YVO}_4$  did not revert to the original phase when the pressure was released [12].

The glow peak temperatures seen in thermoluminescence are sensitive to pressure, and the peak shifts with pressure ( $dT_{\text{peak}}/dp$ ) show a sudden discontinuity in when a phase transition occurs, as noted for TL pressure measurements of KBr [30]. There is an associated shift in the emission spectra.

#### 3.2. Intensity changes and spikes

Quite independently of spectral changes one expects that the luminescence efficiency of different phases will differ. There are thus intensity steps at a phase transition (as seen for the lower temperature peak on Fig. 1). In addition, at the moment that the lattice restructuring occurs, there can be sudden changes in free electron and hole densities (and/or suppression of non-radiative decay pathways) and both these factors will greatly increase the opportunity for luminescence. Consequently one luminescence signature of a phase transition is an intensity spike. This is clearly demonstrated for  $\text{KNbO}_3$ ,

as shown in Fig. 2. This examples show the RL intensity dependence of the material during heating and cooling at low temperature and a similar plot for the higher temperature transition above room temperature, in this case excited during CL [31]. The spectral map of the CL shows that the changes in the emission spectra are far less convenient monitors of the phase change than the intensity step. The example is particular interest as there are clear hysteresis effects, of about 20 degrees in each example. This resolves the apparent discrepancy between published data of two different manufacturers. One used heating, and the other cooling, to characterize their products, but neither emphasised this in their catalogues.

Even more dramatic examples of luminescence intensity spikes were seen in studies of KTP and RTP (potassium and rubidium titanyl phosphate) [32]. Figure 3 includes the initial RL cooling data for RTP which indicates two very dramatic spike features. For comparison are initial cooling data for CL of KTP. Spike features are equally apparent in the CL example but their resolutions, and the relative intensities of signals in each phase, are wavelength dependent. Subsequent heating and cooling cycles effectively remove these features from the luminescence. However, it appears that they are extreme case of hysteresis as reheating the samples to  $\sim 800^\circ\text{C}$  can regenerate them. It is interesting to note that more conventional studies of phase changes with such a hidden hysteresis feature might have overlooked the transitions.

Figure 4 presents low temperature TL from an optical fibre [33]. The material was of interest as after laser

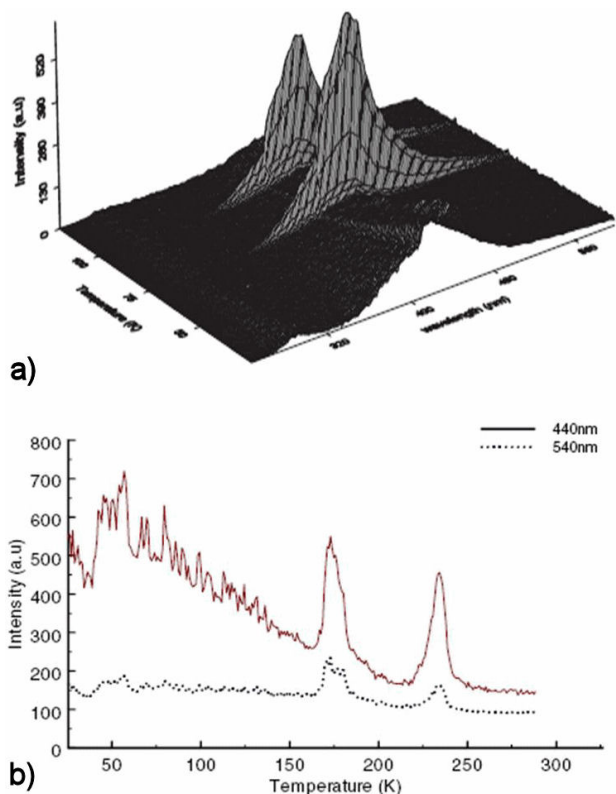


FIGURE 3. Isometric RL data for RTP and CL spectra from KTP during cooling.

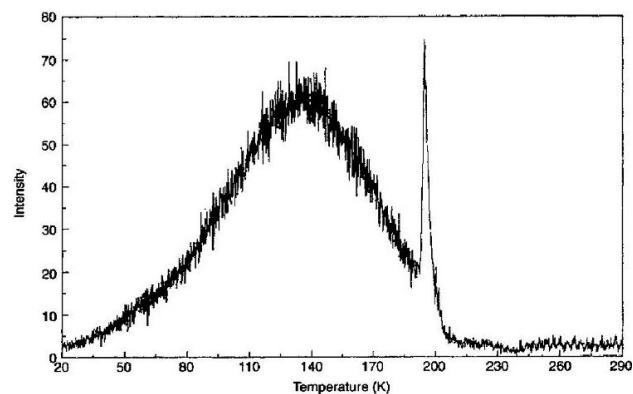


FIGURE 4. TL of a Tm doped germanosilicate optical fibre.

illumination it showed enhanced second harmonic generation but, being a germano-silicate glass fibre; one did not expect crystallinity or phase transitions. Nevertheless there was an intensity spike across the entire emission spectral region near 197K. In our initial publication we suggested that this was evidence for formation of a crystalline glass phase (linked to the SHG data). In hindsight we would instead suggest that this was perhaps evidence for inclusions of  $\text{CO}_2$ . The suggestion of  $\text{CO}_2$  occurs as it sublimates from solid to gas at 197 K at a pressure of  $\sim 1$  bar. The solid to gas phase change implies a volume increase of  $\sim 1,000$  times. This pressure pulse has dramatically modified the rates of electron and hole release that were seen here as a TL signal. A further discussion of  $\text{CO}_2$  nanoparticles in YAG will be made later.

Pulse laser treatments can deposit sufficient energy to allow melting and recrystallization under conditions of extremely rapid cooling. Consequently the restructured material may not be in normal thermodynamic equilibrium and, as with the optical fibre example [33] metastable phases could appear. One such example was noted in pulsed laser treatments of  $\text{CaSO}_4$  rare earth doped radiation dosimeters in which the normal thermoluminescence pattern and emission spectra were displaced and there were recovery steps typical of a phase change [34].

Intensity spike evidence for phase transitions and hysteresis has appeared in data from a number of studies with a variety of materials and RL or CL measurements. The CL examples are particularly interesting as lowering the electron energy excites regions closer to the surface. Surface bonding can differ from the bulk in that there is no constraint for relaxation normal to the surface and thus phase transitions can be enabled more easily than within the interior of the sample. Further, the energy deposited during CL is almost certainly not just a passive probe of the luminescence properties, but it can equally activate ionic motion and thus phase transitions. The overall effect of these features is that CL transitions with low energy electrons (say 6 keV) can show very clean “intensity spike” evidence for phase changes which are less evident for high energy (say 20 keV) electron CL. The actual transition temperatures can differ, as can the scale of the hysteresis. Figure 5 indicates examples of such effects with data taken



with samples from a range of  $\text{KNb}_x\text{Ta}_{1-x}\text{O}_3$  crystals [35]. These compounds have a range of low temperature phase transitions which vary as a function of the Nb to Ta ratio. No detailed discussion of the data is made here but one notes the RL data identified transitions which matched the more familiar X-ray and other “classical” structural analyses. However, the CL results sometimes showed energy dependence and cleaner spike type markers at the lowest temperatures. One must also note that secondary electron emission occurs during CL and this is a function of electron energy. Secondary electrons generate surface charge conditions which induce very strong electric fields (kV/mm) within the surface layer and these fields also have a measurable influence on the phase transition temperature of the  $\text{KNb}_x\text{Ta}_{1-x}\text{O}_3$  crystals. This may be a more general response so further studies should therefore consider how to separate the surface relaxation and impurity effects from the self generated electric fields.

### 3.3. Role of nanoparticles, inclusions and surface impurities

As mentioned above, on viewing the contour map of the luminescence spectral intensity and temperature one frequently recognises a horizontal line feature caused by steeply changing contour map lines, even when there are no obvious movements of the emission spectra. This line definition is evident from the Fig. 6 for signals from a fullerene,  $\text{C}_{60}$ . The example here [36] is for CL stimulated material and is interesting as not only does it register the low temperature phase change noted near 145 K in the short wavelength signals, but also indicates a higher temperature phase event near 245 K in the red emission. Observation of a signal from  $\text{C}_{60}$  is slightly unexpected as this is not an insulator. It is therefore possible that one is sensing signals from contaminants, such as solvents used in the sample preparation. CL is a surface analysis and this may account for the 245 K signals since, if there is water vapour trapped on the surface, there is the possibility of this undergoing a phase transition from solid to vapour at this temperature (as note for the ice phase diagram in a vacuum system). The fullerene example underlines the fact that impurity signals can act as probes of different types of transition. Such signals offer an interesting insight into the scale of how surface water or inclusions are bonded into, or on, a material. If one is sensing a “classical” bulk phase transition of such impurities one must ask how large is the assembly of ions which allow this to behave as a bulk material. For insulators, such as water or  $\text{CO}_2$ , one may infer from the current examples that inclusions on a nanoparticle scale are still behaving in a pseudo-bulk manner in terms of transition temperature. By contrast the evidence from earlier work with metals is that at least the melting temperature is extremely sensitive to nanoparticle size and melting points fall from say 1,000 to below  $400^\circ\text{C}$  as the metal particle size is decreased.

Many features are influenced by changes of inclusions, precipitates or absorbates in which the spectra are defined

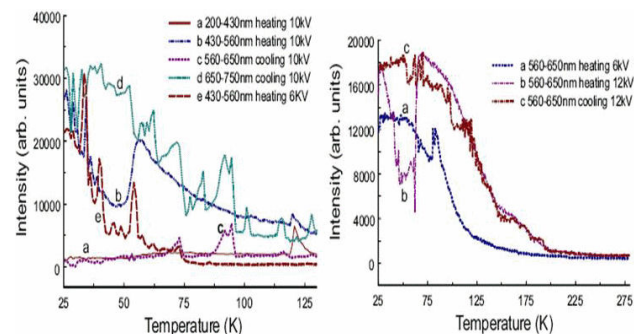


FIGURE 5. Examples of CL from a range of  $\text{KNb}_x\text{Ta}_{1-x}\text{O}_3$  crystals. The features show unexpected complexity in the low temperature phase transitions.

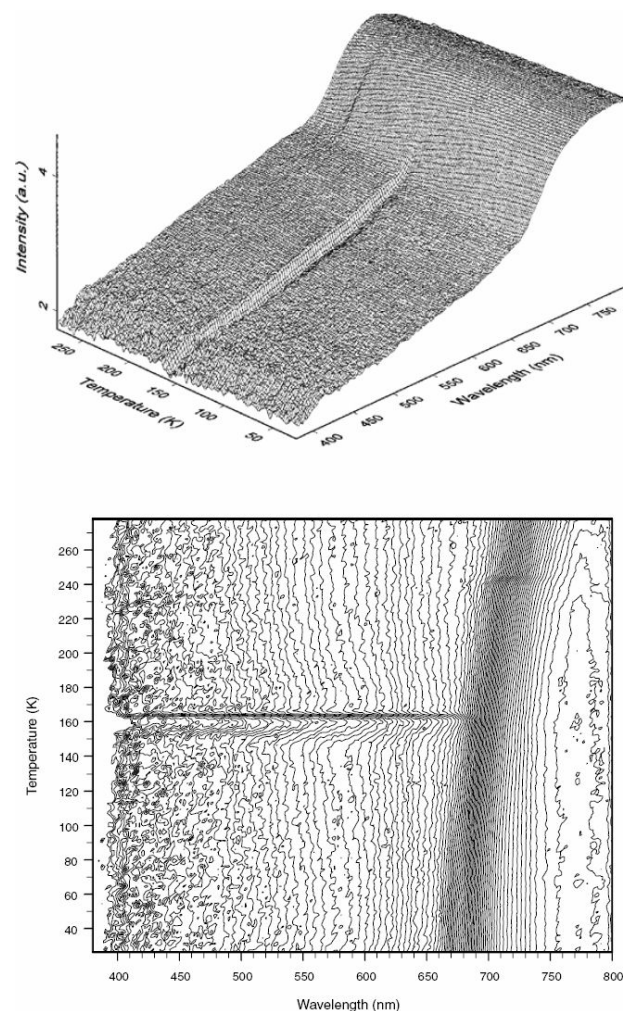


FIGURE 6. Detection of phase transitions from the intensity steps for data from a fullerene.

by the host, but modified in intensity, wavelength and lifetime from the impurities. For example, as seen in Fig. 7 from Nd:YAG [22], the blue Nd line positions are displaced discontinuously near 197 K. As for the glass fibre example, shown in Fig. 4, this is again attributed to crystal field changes caused by lattice expansion associated to increased

pressure driven by sublimation of nanoparticles of  $\text{CO}_2$  near 200 K. X-ray analysis of powder from this crystal showed the lattice remained cubic, but with a discontinuous lattice parameter compression to 1.2007 nm compared with a normal value of 1.2013 nm in this temperature region. Note there may be small offsets in the temperature values for the X-ray powder data.

The smaller higher temperature feature near 230 K may be associated to the presence of surface water/ice. Water is a ubiquitous contaminant and uptake of surface water over several days can modify the Nd CL emission spectra [37].

Water nanoparticles, in the form of inclusions, and/or surface or grain boundary layers, has been inferred from many

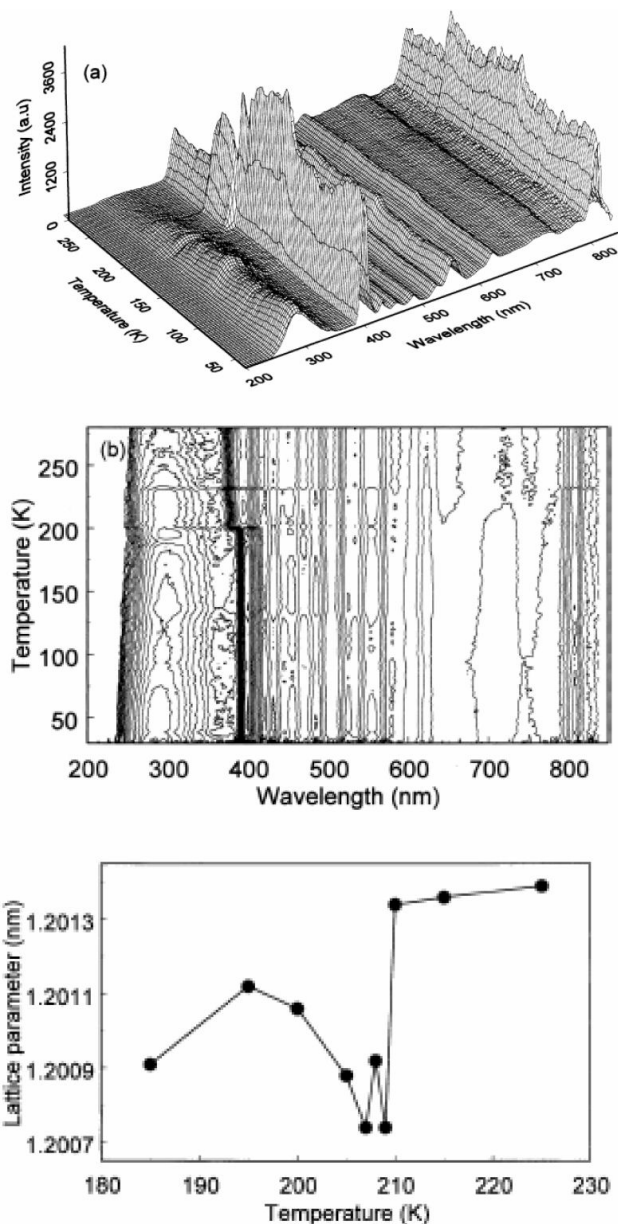


FIGURE 7. Note the wavelength shift for the blue Nd line from Nd:YAG. Lattice parameter data show an anomaly at the same temperature region.

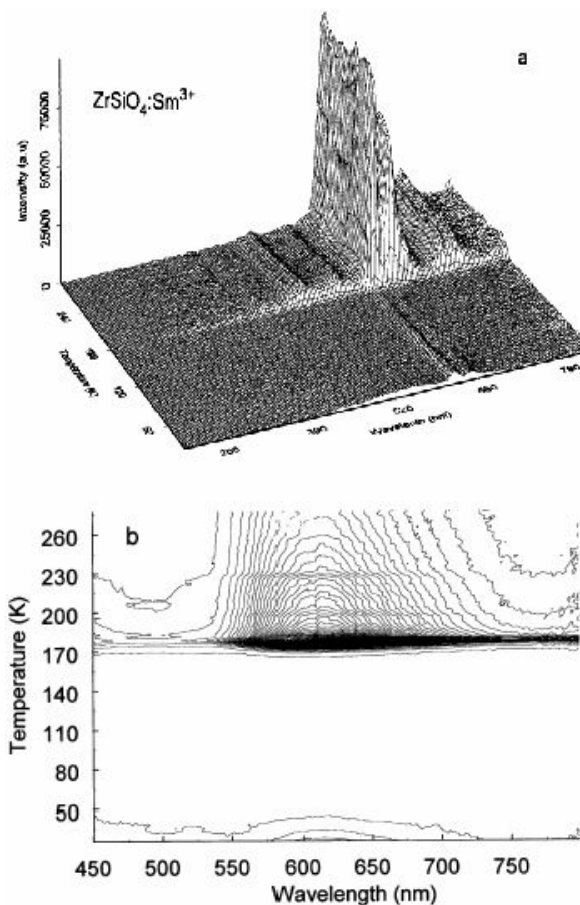


FIGURE 8. Luminescence from zircon with intensity steps attributed to phase changes from ice nanoparticles.

types of sample since many RL and CL signals of the host lattice undergo a very major intensity step near 170 K, which corresponds to the cubic to hexagonal phase transition of ice [22,23,38]. In some materials the association with near surface water has been cleanly demonstrated by heat treatments which drive off the water (and the luminescence intensity step is removed) followed by exposure to steam (which reintroduces it). The 170 K event is shown in the example of Fig. 8 for CL signals from zircon.

Zircon data are also surprising in that the main low temperature TL peak changes temperature monotonically with the size of rare earth dopants [29]. This is a common phenomenon and is documented for other TL systems. In the case of  $\text{LaF}_3$  the low temperature peak moves  $\sim 15$  degrees for the range of rare earth dopants [40], 20 degrees in molybdates [41] and 30 degrees in phosphates [42]. By contrast, in zircon the movement is more than 150 degrees [39]. A simple explanation is that the rare earth ions are not simply accommodated on distorted lattice sites, but instead result in precipitations of RE silicates. These would therefore have a far larger range of variation in lattice parameter and so result in larger changes in bond energy and temperature of the glow peak. Luminescence can therefore offer evidence for precipitate phase formation.

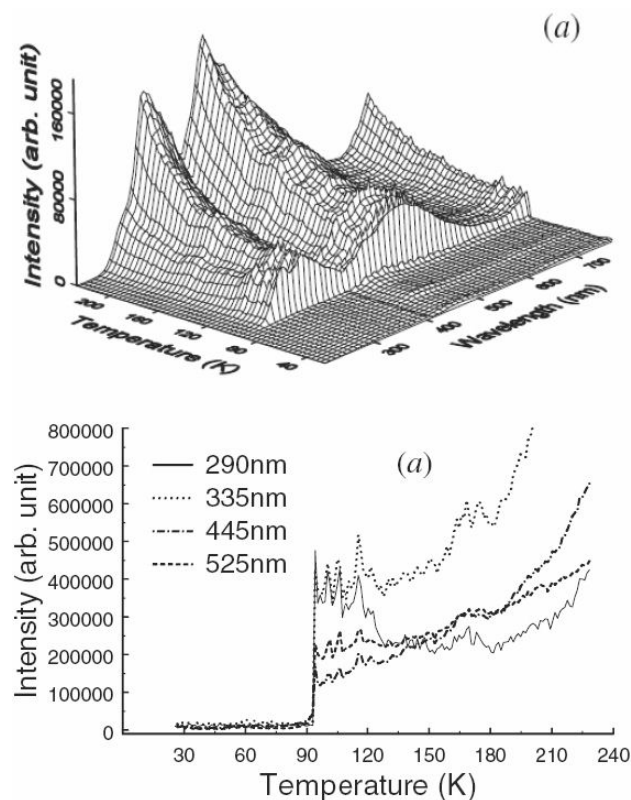


FIGURE 9. CL luminescence from a superconductor, a-(Bi,Pb)-2223/Ag tape. Note the intensity steps near the superconducting transition temperature.

The trapped impurity signals are not confined to the surface and many examples are seen with RL, implying that they are from bulk material. A series of intensity discontinuities were noted with low grade crystals of MgO doped with Cr in which the red chromium emission band underwent both intensity steps and wavelength displacements at a number of temperatures [24]. The temperature values were tentatively linked to phase transitions of trapped gas, such as  $N_2$  and  $O_2$ , as the event lines matched their solid/liquid and liquid/gas phase transitions. For the same samples there were differences in the direction of the wavelength shifts from RL and CL data. This is not unreasonable since within the bulk these phase changes involve expansions and increases in pressure with compression of the neighbouring MgO lattice. By contrast the CL probes the surface where the pressure changes can result in a surface expansion of the lattice and a corresponding lattice expansion.

Trapped gas signals were similarly noted from alumina samples prepared by pulse laser deposition in an argon atmosphere [43]. The intensity steps match the phase transition temperature of argon. These examples are interesting because they indicate that such trapped gas is precipitating into bubbles, rather than being randomly dispersed.

Within the category of inclusions one may also include mention of chemically bonded water and indeed during the heating of water rich silica gel the luminescence signals change as the bonded water is liberated and the samples

switch from pink to blue. Loss of water of crystallization in silica gel and irreversible changes in  $Na_2SO_4$  result in steps in the luminescence signals [44].

### 3.4. Luminescence detection of superconducting transitions

Superconductors may offer luminescence signals directly from the host material or from impurities such as surface oxides or sulphides. Once the host material is cooled through a superconducting phase transition the optical signals can be totally modified [45]. Figure 9 shows signals from the surface of Bi/Pb -2223 Ag tape [45]. There is a strong luminescence CL signal which ceases when the material switches to a superconducting state. Visually one sees that the electron beam is displaced from the sample to the adjacent copper support as magnetic flux is excluded from the superconductor. One notes that there are higher temperature spikes suggesting that some grains of the material may demonstrate even higher transition temperatures up to say 120 K instead of  $\sim 90$  K. Phase transitions occur for the scintillator  $PbF_2$  [46].

### 3.5. Influence of surface ion implantation on bulk properties

Intuitively one assumes that ion beam implantation is a surface effect in which there is doping of the host material and, for high doses, some sputtering and changes in composition of the implanted layer. There will additionally be stresses which modify the implanted crystal and the stress fields will not be confined to the implant zone. At very high implant concentrations the lattice is no longer thermodynamically stable and standard behaviour includes relaxation into new structures, new compounds and/or precipitation of sub-phases or nanoparticles. Indeed such events are well documented in the ion implantation literature and in the case of luminescent nanoparticles in semiconductors and silica the emission spectra change progressively with the size of the nanoparticles. The interpretations of the changes in signal are often controversial at the detailed level but nevertheless the signals are monitors of the implanted volume. In the case of optical waveguides formed by ion implantation of light ions to form a low refractive index damage layer to separate the waveguide from the bulk, the guide is stressed relative to the bulk material [19,47]. Hence in waveguides formed in say Nd:YAG the emission spectra, relative line intensities, transition probabilities and emission wavelengths are perturbed relative to those of the bulk material. Such changes are to be expected and are well documented for a range of ion implanted laser waveguides [48].

A far less predictable outcome of the surface implantation is that the stress fields will induce phase transitions which propagate throughout the bulk material. Several materials are suitable candidates for this instability to their choice of phase and potential examples include strontium titanate, zinc oxide, bismuth germanate or silicon carbide. In each case structural



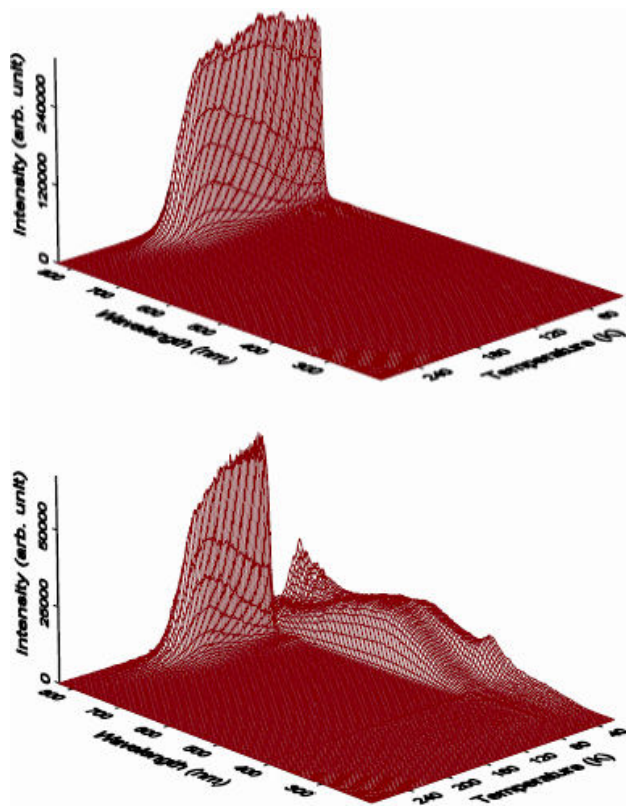


FIGURE 10. Luminescence from as received and ion implanted strontium titanate.

analyses have revealed that such materials can vary in their stoichiometry, include a number of stable or metastable phases, and that relaxations or phase transitions are sensitive to impurities and/or stress. Thus, in hindsight, implants into these materials may show bulk luminescence signals which indicate phase variations as the result of surface treatments. The example of  $\text{SrTiO}_3$  fits this pattern and Fig. 10 contrasts the RL signals of pure and ion implanted samples [49]. The implant depth is merely  $\sim 100\text{nm}$  whereas the bulk material is  $\sim 1\text{mm}$  thick. Thus the optical signals reveal the result of bulk relaxation and the intensity steps generated in the implanted samples match known phase transitions of  $\text{SrTiO}_3$ . The results differ between samples of different purity but are insensitive to the choice of implant. There is evidence for such relaxations and phase changes in RL [49], CL [50] and TL [51]. Similar unusual data (unpublished) have been seen for ZnO and one suspects that this is a far more general occurrence.

#### 4. Summary

Detection of phase transitions via changes in luminescence signals has been demonstrated many times over the last 40 years but the brief selection of examples shown here emphasise that not only is it a sensitive and powerful approach, but also it is widely applicable to a range of materials, not just insulators. A major advantage of the method appears to be that it is extremely suitable for initial rapid surveys in searches for phase transitions. Less obvious is that the signals reveal differences between bulk and surfaces and the presence of impurities, precipitates and nanoparticles. Such inclusions dramatically influence the luminescence of the host. In terms of detectable responses one can summarise features which mark a transition event as follows:-

1. The transition probabilities change, giving a discontinuity in intensity.
2. Changes in electron and hole densities add a luminescence spike signature.
3. The emission spectra alter between phases.
4. Phase transitions of inclusions generate effects on the host luminescence.
5. Polarization responses will change.
6. There are discontinuities in luminescence lifetimes and linewidths.
7. Rare earth transitions are particularly sensitive to the site symmetry.
8. Second harmonic generation will respond to stress and structural changes.
9. Ion implantation in the surface can induce relaxations and phase changes in the bulk material.

To conclude, the luminescence literature related to phase transitions is sparse and relatively ignored but it is a simple and productive approach for detection of bulk crystal first order transitions, “soft” transitions, phase changes of inclusions and nanoparticles, and irreversible or decomposition events. Combinations of excitation methods indicate that far more complexity exists than had previously been discussed and the subject area has considerable unexplored depth of interesting phenomena. Further examples are cited in a recent extended review [52].

1. C.N.R. Rao and K.J. Rao, *Phase Transitions in Solids* (McGraw-Hill, New York, 1978).
2. W. Hayes and A.M. Stoneham, *Defects and Defect Processes in Non-metallic Solids* (Wiley, New York, 1985).

3. F. Agullo-Lopez, C.R.A. Catlow, and P.D. Townsend, *Point Defects in Materials* (Academic Press, London, 1988).
4. W.F. Zhang, Z. Yin, M.S. Zhang, Z.L. Du, and W.C. Chen, *J. Phys Condensed Matter* **11** (1999) 5655.

5. C. Burda *et al.*, Chapter 7 in *Characterization of Nanophase Materials*, Ed: Zhong Lin Wang (Wiley-VCH Verlag GmbH, 2000) p. 197.
6. L.A. Boatner and C.W. White, *Nucl Inst Methods B* **178** (2001) 7.
7. E. Courtens, *Phys. Rev. Lett.* **29** (1972) 1380.
8. E. Salje and K. Viswanathan, *Acta Cryst.* **A31** (1975) 356.
9. T.A. Kuketaev, *Opt. Spectrosc.* **59** (1985) 337.
10. C.S. Yoo, H.B. Radousky, N.C. Holmes, and N.M. Edelstein, *Phys. Rev. B* **44** (1991) 830.
11. B.J. Baer and H.G. Drickamer, *J. Phys. Chem.* **95** (1991) 9477.
12. G. Chen, N.A. Stump, R.G. Haire, J.R. Peterson, and M.M. Abraham, *Solid State Commun.* **84** (1992) 313.
13. M.C. Marco de Lucas *et al.*, *Rad. Eff. Def. Solids* **135** (1995) 19.
14. J. Kroupa and A. Fuith, *Phys. Rev. B* **48** (1993) 4119.
15. R. Subramanian, L.K. Patterson, and H. Levanon, *Chem Phys Letts* **93** (1982) 578.
16. O. Zelaya-Angel, A.E. Esparza-Garcia, C. Falcony, R. Lozada-Morales and R. Ramirez-Bon, *Solid state comm.* **94** (1995) 81.
17. J. Menniger, U. Jahn, O. Brandt, H. Yang, and K. Ploog, *Phys. Rev. B* **53** (1996)
18. L. Zlatkevich, *Radiothermoluminescence and Transitions in Polymers* (Springer, New York, 1987).
19. P.D. Townsend, P.J. Chandler, and L. Zhang, *Optical effects of ion implantation* (Cambridge University Press, Cambridge, 1994).
20. P.D. Townsend *et al.*, *J. Phys.: Condensed Matter* **13** (2001) 2211.
21. P.D. Townsend, *Rad. Eff.* **155** (2001) 11.
22. M. Maghrabi, P.D. Townsend, and G. Vazquez, *J Phys: Condensed Matter* **13** (2001) 2497.
23. K. Kurt, V. Ramachandran, M. Maghrabi, P.D. Townsend, and B. Yang, *J Phys Condensed Matter* **14** (2002) 4319.
24. M. Maghrabi, F. Thorne, and P.D. Townsend, *Nucl Inst Methods B* **191** (2002) 181.
25. W Becker, *Advanced Time-correlated single photon counting techniques* (Springer Berlin, 2005).
26. D.S. Betts, L. Couturier, A.H. Khayrat, B.J. Luff, and P.D. Townsend, *J. Phys. D* **26** (1993) 843; *ibid J. Phys. D* **26** (1993) 849.
27. G. Kitis and J.W.N. Tuyn, *J. Phys. D* **31** (1998) 2065; *ibid Rad Protect Dosim* **84** (1999) 371.
28. P.D. Townsend, A.P. Rowlands, and G. Corradi, *Rad. Measur.* **27** (1997) 31.
29. A. Ege, Y. Wang, and P.D. Townsend, *Nucl Insts and Methods A* **576** (2007) 411.
30. B.J. Baer and H.G. Drickamer, *J Phys Chem* **95** (1991) 9477.
31. B. Yang, P.D. Townsend, and M. Maghrabi, *J. Modern Opt.* **48** (2001) 319.
32. C.V. Kannan *et al.*, *J Phys Condensed Matter* **15** (2003) 7599.
33. P.D. Townsend, R.A. Wood, W.S. Brockelsby, R.S. Brown and J.E. Townsend, *Rad. Protect Dosimetry* **65** (1996) 363.
34. T. Karali, A.P. Rowlands, P.D. Townsend, M. Prokic, and J. Olivares, *J Phys D* **31** (1998) 754.
35. R. Kibar, P.J.T. Nunn, P.D. Townsend, Y. Wang, and L.A. Boatner, *Phys stat sol (c)* **4** (2007) 905.
36. A.P. Rowlands *et al.*, *J. Phys Condensed Matter* **12** (2000) 7869.
37. A. Peto, P.D. Townsend, D.E. Hole, and S. Harmer, *J. Modern Optics* **44** (1997) 1217.
38. P.D. Townsend, M. Maghrabi, and B. Yang, *Nucl. Inst. Methods B* **191** (2002) 767.
39. T. Karali, N. Can, P.D. Townsend, A.P. Rowlands, and J. Hanchar, *Amer Mineralogist* **85** (2000) 668.
40. B. Yang, P.D. Townsend, and A.P. Rowlands, *Phys Rev B* **57** (1998) 178.
41. L.H. Brixner, P.E. Bierstedt, A.W. Sleight, and M.S. Licis, *Mater Res Bull* **6** (1971) 545.
42. C. Ting and H. Guang-Yen, *Acta Phys Sin. (Jpn)* **35** (1986) 1521.
43. Z. Wu *et al.*, *Nucl. Instr. and Meth. B* **191** (2002) 121.
44. A.P. Rowlands, A.K. Tyagi, T. Karali, and P.D. Townsend, *Rad. Protect Dosimetry* **100** (2002) 55.
45. B. Yang, P.D. Townsend, and W. Lin, *J. Modern Optics* **51** (2004) 619.
46. B. Yang and P.D. Townsend, *Physica Status Solidi (a)* **196** (2003) 477.
47. Feng Chen, Xue-Ling Wang, and Ke-Ming Wang, *Optical materials* **29** (2007) 1523.
48. P.D. Townsend, *Proc of Laser Technologies and Lasers* (Plovdiv, 2005) p. 32.
49. B. Yang, P.D. Townsend, and R. Fromknecht, *Nucl Inst Methods B*, **217** (2004) 60.
50. B. Yang, P.D. Townsend, and R. Fromknecht, *J Phys Condensed Matter* **16** (2004) 8377.
51. B. Yang, P.D. Townsend, and R. Fromknecht, *Nucl Inst Methods B*, **226** (2004) 549.
52. P.D. Townsend, B. Yang, and Y. Wang, *Contemporary Physics*, (2008, *in press*).